

Stress-assisted magnetic-field-induced strain in Ni-Fe-Ga-Co ferromagnetic shape memory alloys

著者	及川 勝成
journal or publication title	Applied Physics Letters
volume	90
number	6
page range	062505-1-062505-3
year	2007
URL	http://hdl.handle.net/10097/34941

Stress-assisted magnetic-field-induced strain in Ni–Fe–Ga–Co ferromagnetic shape memory alloys

H. Morito,^{a)} A. Fujita, K. Oikawa, and K. Ishida

Department of Materials Science, Graduate School of Engineering, Tohoku University, Aoba-yama 6-6-02, Sendai 980-8579, Japan

K. Fukamichi and R. Kainuma

Institute of Multidisciplinary Research for Advanced Materials, Tohoku University, Katahira 2-1-1, Sendai 980-8577, Japan

(Received 9 November 2006; accepted 8 January 2007; published online 5 February 2007)

To obtain a large strain for Ni–Fe–Ga ferromagnetic shape memory alloys, the Curie temperature was increased by adding Co, and the magnetic-field-induced strain (MFIS) has been investigated under static stresses. The magnetocrystalline anisotropy constant K is increased by the addition of Co, and Ni₄₉Fe₁₈Ga₂₇Co₆ alloy gives a relatively large value of 1.15×10^6 erg/cm³ at 300 K. From the stress-strain curves for this alloy, the twinning stress is estimated to be 8–9 MPa. Consequently, the Ni₄₉Fe₁₈Ga₂₇Co₆ alloy exhibits a large MFIS of about 8.5% at room temperature under a static compressive stress of about 8 MPa. © 2007 American Institute of Physics.

[DOI: 10.1063/1.2450667]

Ferromagnetic shape memory alloys (FSMAs) having a large magnetic-field-induced strain (MFIS) have attracted much attention, because they are promising as magnetic-controlled actuators and sensors. Large MFISs have been observed in martensite phases of Ni₂MnGa alloys^{1,2} and other FSMAs.^{3–9} However, intrinsic high brittleness of Ni₂MnGa is a disadvantage for practical applications. Therefore, developments of ferromagnetic shape memory alloys with excellent mechanical properties are strongly expected.

The MFIS is explained by the rearrangement of martensite variants due to an external magnetic field.¹ When the magnetocrystalline anisotropy energy is larger than the energy driving variant boundaries, the angle between magnetization and the applied magnetic field directions is lowered by not only the independent rotation of magnetization but also the variant rearrangement in order that the magnetic easy axis is aligned parallel to the magnetic field direction.^{1,10} Since the MFIS is caused by the reorientation of the martensite variants, the behavior of MFIS is affected by magnetocrystalline anisotropy as well as mobility of variant boundaries. The magnetocrystalline anisotropy energy is required to be larger than the energy to drive the variant boundaries.

Recently, Ni–Fe–Ga Heusler-type alloys^{11–16} have drawn attention as practical FSMAs. It has been reported that the ductility of Co–Ni–Al alloy can be increased by introducing a small amount of γ (A1) phase.¹⁷ In a similar way, therefore, the Ni–Fe–Ga system is expected to have excellent mechanical properties. However, in the ternary Ni–Fe–Ga alloys, the magnetocrystalline anisotropy constant in the vicinity of room temperature is not so large because of a low Curie temperature.¹⁶ To overcome such a practical problem, the increase of the Curie temperature has been searched by adding Co.^{18–20} As a result, the Curie temperature is effectively increased¹⁸ and hence the single-variant martensite phase of Ni₅₂Fe₁₈Ga₂₇Co₃ exhibits a large MFIS of about 0.7% at 300 K.²¹ The reason why the magnitude of the present MFIS is smaller than the 10% strain of Ni₂MnGa (Ref. 2) is that

the magnetocrystalline anisotropy constant is still small in Ni₅₂Fe₁₈Ga₂₇Co₃.

To obtain a large MFIS in the vicinity of room temperature, in the present letter, we have tried to increase the magnetocrystalline anisotropy constant by controlling the Co concentration and then investigated the MFIS under static compressive stresses.

The single crystals of Ni_{55-x}Fe₁₈Ga₂₇Co_x ($x=3-6$) were grown by an optical floating-zone method under a helium atmosphere. The single crystal specimens were annealed at 1433–1473 K for 2 days to homogenize and followed by quenching in ice water. After the homogenization, they were additionally heat treated at 873 K for 1–3 days to make the antiphase domain large and heat treated at 673 K for 1 day to achieve a high degree of atomic order in the Heusler structure. Although the martensitic transformation starting temperature M_s decreases from 331 to 300 K with increasing Co content x from 3 to 6, the Ni_{55-x}Fe₁₈Ga₂₇Co_x ($x=3-6$) single crystal samples are in a martensite phase at room temperature. The crystallographic orientations were determined from the electron backscattering diffraction patterns. The cubic specimens in the parent phase were trimmed so that the $\langle 100 \rangle_P$ (P : parent) directions are parallel to the faces. The $\langle 100 \rangle_P$ a axis in the $L2_1$ cubic parent phase corresponds to either the $\langle 110 \rangle_M$ or the $2 \times \langle 001 \rangle_M$ (M : martensite) c axis in the $L1_0$ tetragonal martensite phase. In order to obtain the single-variant specimen, uniaxial compressive stresses were applied to the $[010]_P$ and $[001]_P$ directions in the martensite phase of the above-mentioned single crystals. After applying compressive stress, the c axis of the $L1_0$ unit cell is oriented to the $[100]_P$ direction. The magnetization was measured up to 20 kOe with a superconducting quantum interference device magnetometer. The MFIS was measured with an extensometer under a compressive stress in magnetic fields.

The magnetocrystalline anisotropy constant K in the single-variant specimen was determined from the magnetization curves measured along the c axis and c plane of the $L1_0$ structure. The magnetization curves at $T=300$ K for the Ni_{55-x}Fe₁₈Ga₂₇Co_x alloys ($x=3-6$) are shown in Fig. 1. The

^{a)}Electronic mail: a4td5309@stu.material.tohoku.ac.jp

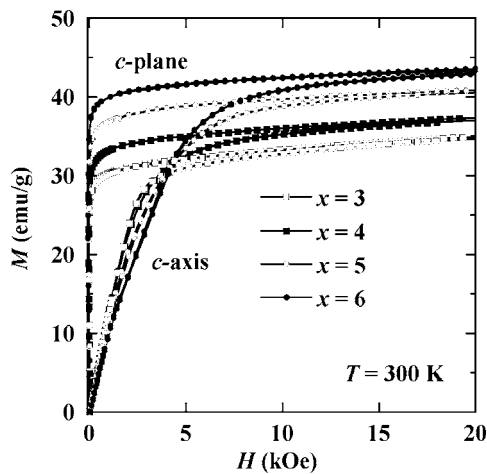


FIG. 1. Magnetization curves along the c -axis and c -plane directions for the single-variant martensite phase in the $\text{Ni}_{55-x}\text{Fe}_{18}\text{Ga}_{27}\text{Co}_x$ ($x=3-6$) alloys.

curves for the c plane are easily saturated, whereas the curves for the c axis are hardly saturated. These results indicate, therefore, that the $\text{Ni}_{55-x}\text{Fe}_{18}\text{Ga}_{27}\text{Co}_x$ alloys ($x=3-6$) show a uniaxial magnetocrystalline anisotropy, and the c axis is the hard axis of magnetization. After correcting the demagnetizing field, the value of K was evaluated from the area between the easy and hard magnetization curves. Shown in Fig. 2 are the saturation magnetization M_{sat} and the concentration dependences of K for the $\text{Ni}_{55-x}\text{Fe}_{18}\text{Ga}_{27}\text{Co}_x$ ($x=3-6$) alloys in the martensite phase. The values of M_{sat} and K increase from 33 to 43 emu/g and 0.45×10^6 to 1.15×10^6 erg/cm³, respectively, with increasing Co content x from 3 to 6. Therefore, the increase of T_C by the addition of Co effectively enhances the saturation magnetization and the magnetocrystalline anisotropy constant.

The variant boundary motion under the magnetic field is the identical motion under the stress. Therefore, the mobility of the variant boundaries is related to the twinning stress,² that is, low twinning stress results in a high mobility of the variant boundaries. As a representative example, the stress-strain curves at room temperature for the $\text{Ni}_{49}\text{Fe}_{18}\text{Ga}_{27}\text{Co}_6$ alloy along the $\langle 100 \rangle_P$ directions are presented in Fig. 3. The reverse transformation starting temperature A_s is 303 K; therefore the sample is in the martensite phase at room tem-

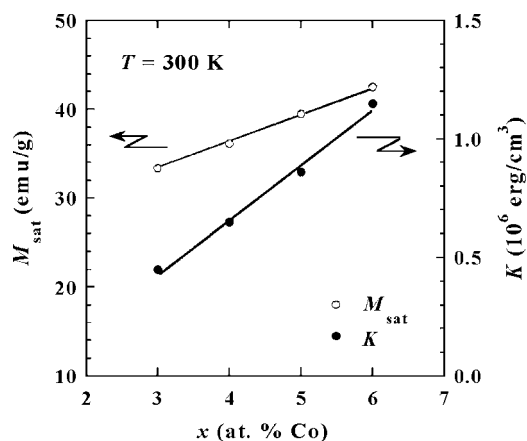


FIG. 2. Concentration dependence of saturation magnetization M_{sat} and the magnetocrystalline anisotropy constants K at 300 K for the $\text{Ni}_{55-x}\text{Fe}_{18}\text{Ga}_{27}\text{Co}_x$ ($x=3-6$) alloys in the martensite phase.

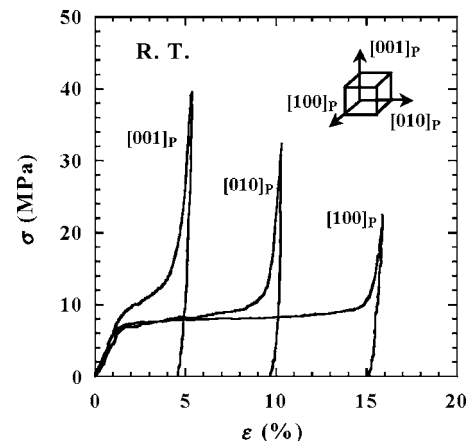


FIG. 3. Compressive stress-strain curves along the $\langle 100 \rangle_P$ directions at room temperature in the martensite phase for the $\text{Ni}_{49}\text{Fe}_{18}\text{Ga}_{27}\text{Co}_6$ alloy.

perature. Although the compressive stresses were applied to the martensite phase, the expression of crystal directions is related to that of the parent phase. In the first cycle, the compressive stress was applied along the $[001]_P$ direction. The variant rearrangement was initiated above the applied twinning stress σ_{tw} of 10–14 MPa, which corresponds to the plateau, and the obtained twinning strain ϵ is about 4% in the first cycle. In the second cycle, the compressive stress was applied along the $[010]_P$ direction. The variant rearrangement takes place at a much lower stress of 8–10 MPa. Furthermore, the value of the remaining strain is increased up to 10% and the sample becomes in a single-variant state. For the evaluation of the variant boundary mobility, the compressive stress was applied along the $[100]_P$ direction of the single-variant sample. Stress of 8–9 MPa for the variant rearrangement and strain of 15% are achieved in the third cycle. The value of K is exactly equal to the magnetic driving force applied to the variants; therefore, K has to exceed or be of the same order as the mechanical energy $\epsilon\sigma_{\text{tw}}$ consumed for the variant rearrangement.² From the x-ray diffraction, it was confirmed that the $14M$ and nonmodulated $L1_0$ structures coexist in $\text{Ni}_{49}\text{Fe}_{18}\text{Ga}_{27}\text{Co}_6$ alloy.¹⁸ However, under the stress, the $L1_0$ structure becomes more stable,¹⁶ and hence the high twinning stress cuts off the appearance of the large MFIS.

A static stress aiding the magnetic field was used to achieve a large MFIS, that is, the magnetic field was applied under a compressive stress. Before applying the magnetic field, compressive stress of about 8 MPa was applied along the c axis ($[100]_P$) direction which is the hard magnetic direction. As a result, shrinkage of 5% was observed as seen in Fig. 4(a). The magnetic field was then applied parallel to the c axis direction. As demonstrated in Fig. 4(b), during the application of the magnetic field, a steep shrinkage caused by the variant rearrangement due to the magnetization rotation is observed around $H=4$ kOe, and the maximal strain reaches 8.5% in a field of 10 kOe. After applying the magnetic field, the easy plane in the variant is aligned parallel to the magnetic field direction and the sample becomes in a near single-variant state with the easy plane along the field direction. By applying a uniaxial stress along the $[100]_P$ direction, the transformation always occurred from the single-variant to the multivariant state because the c axis of the martensite phase orients along the two equivalent directions, i.e., $[010]_P$ and $[001]_P$. In the present alloy system, however,

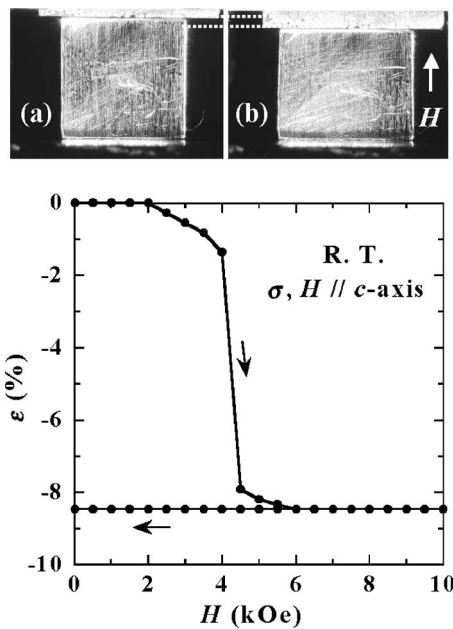


FIG. 4. Magnetic-field-induced strain ϵ measured parallel to the direction of magnetic field H applied along the c axis at room temperature for the $\text{Ni}_{49}\text{Fe}_{18}\text{Ga}_{27}\text{Co}_6$ single-variant specimen under stress of about 8 MPa. The above two photographs show the shape change of the specimen (a) before and (b) during application of a magnetic field.

the transformation occurs from the single-variant to the other single-variant state. The detail mechanism is not clear at the moment, but a preferential nucleation of one variant takes place in the present alloys. The variant rearrangement driven by the magnetic field is discussed quantitatively by introducing the magnetic shear stress τ_{mag} acting across the twinning plane.²² For the variant rearrangement by applying a magnetic field, the value of τ_{mag} should be larger than the mechanical shear stress τ_{req} required for the variant rearrangement. The value of τ_{mag} is expressed as $|K|/s$, where s is the corresponding twinning shear. The twinning plane is $\{101\}_P$ for the Ni–Fe–Ga–Co alloys; therefore, the value of twinning shear is estimated from $s = \{1 - (c/a)^2\}/(c/a)$. Then, the value of s is calculated from the lattice parameters.^{7,18} For the $\text{Ni}_{49}\text{Fe}_{18}\text{Ga}_{27}\text{Co}_6$ alloy, the value of τ_{mag} is evaluated as $\tau_{\text{mag}} = 0.3$ MPa. Taking into account the twinning plane and the Schmid factor, $\tau_{\text{req}} (= 0.5\sigma_{\text{tw}})$ is estimated to be 4.0–4.5 MPa from the stress-strain curves. In this case, shear stress of $\tau \sim 4$ MPa was applied before applying a magnetic field. Therefore, τ_{req} is decreased to $\tau_{\text{req}} < 0.5$ MPa, which corresponds to the plateau slope in the stress-strain curve. By applying a magnetic field, magnetic shear stress of about 0.3 MPa is added, and the mechanical shear stress, equivalent to the variant rearrangement, is obtained.

In conclusion, the increase of the Curie temperature T_C by the Co addition effectively increases the magnetocrystalline anisotropy constant K . The value of K for the present

$\text{Ni}_{49}\text{Fe}_{18}\text{Ga}_{27}\text{Co}_6$ alloy at $T = 300$ K is evaluated to be 1.15×10^6 erg/cm³, being nearly equivalent to that of Ni_2MnGa alloy.² From these results, the magnetocrystalline anisotropy energy is enhanced by adjusting the concentration of Co in the Ni–Fe–Ga alloys. In the $\text{Ni}_{49}\text{Fe}_{18}\text{Ga}_{27}\text{Co}_6$ alloy, the variant rearrangement associated with the magnetization rotation was observed, and the maximal strain of 8.5% was confirmed under a compressive stress of about 8 MPa. From these results, it has been revealed that the present Ni–Fe–Ga–Co ferromagnetic shape memory alloys are promising as large MFISs assisted by static compressive stresses.

The authors wish to thank Y. Sutou, T. Ota, and T. Takagi for their experimental support. A part of the present study was supported by the Grant-in-Aids for Core Research for Evolutional Science and Technology (CREST), Scientific Research from the Ministry of Education, Science, Sports and Culture, Japan, and the Research Fellow of the Japan Society.

¹K. Ullakko, J. K. Huang, C. Kantner, R. C. O'Handley, and V. V. Kokorin, *Appl. Phys. Lett.* **69**, 1966 (1996).

²A. Sozinov, A. A. Likhachev, N. Lanska, and K. Ullakko, *Appl. Phys. Lett.* **80**, 1746 (2002).

³R. D. James and M. Wuttig, *Philos. Mag. A* **77**, 1273 (1998).

⁴T. Kakeshita, T. Takeuchi, T. Fukuda, M. Tsujiguchi, T. Saburi, R. Oshima, and S. Muto, *Appl. Phys. Lett.* **77**, 1502 (2000).

⁵A. Fujita, K. Fukamichi, F. Gejima, R. Kainuma, and K. Ishida, *Appl. Phys. Lett.* **77**, 3054 (2000).

⁶K. Oikawa, L. Wulff, T. Iijima, F. Gejima, T. Ohmori, A. Fujita, K. Fukamichi, R. Kainuma, and K. Ishida, *Appl. Phys. Lett.* **79**, 3290 (2001).

⁷K. Oikawa, T. Ota, F. Gejima, T. Ohmori, R. Kainuma, and K. Ishida, *Mater. Trans.* **42**, 2472 (2001).

⁸H. Morito, A. Fujita, K. Fukamichi, R. Kainuma, K. Ishida, and K. Oikawa, *Appl. Phys. Lett.* **81**, 1657 (2002).

⁹M. Wuttig, J. Li, and C. Craciunescu, *Scr. Mater.* **44**, 2393 (2001).

¹⁰R. C. O'Handley, *J. Appl. Phys.* **83**, 3263 (1998).

¹¹K. Oikawa, T. Ota, Y. Sutou, T. Ohmori, R. Kainuma, and K. Ishida, *Mater. Trans.* **43**, 2360 (2002).

¹²K. Oikawa, T. Ota, T. Ohmori, Y. Tanaka, H. Morito, A. Fujita, R. Kainuma, K. Fukamichi, and K. Ishida, *Appl. Phys. Lett.* **81**, 5201 (2002).

¹³Z. H. Liu, M. Zhang, Y. T. Cui, Y. Q. Zhou, W. H. Wang, G. H. Wu, X. X. Zhang, and G. Xiao, *Appl. Phys. Lett.* **82**, 424 (2003).

¹⁴H. Morito, A. Fujita, K. Fukamichi, T. Ota, R. Kainuma, K. Ishida, and K. Oikawa, *Mater. Trans.* **44**, 661 (2003).

¹⁵H. Morito, A. Fujita, K. Fukamichi, R. Kainuma, K. Ishida, and K. Oikawa, *Appl. Phys. Lett.* **83**, 4993 (2003).

¹⁶Y. Sutou, N. Kamiya, T. Omori, R. Kainuma, K. Ishida, and K. Oikawa, *Appl. Phys. Lett.* **84**, 1275 (2004).

¹⁷R. Kainuma, M. Ise, C.-C. Jia, H. Ohtani, and K. Ishida, *Intermetallics* **4**, S151 (1996).

¹⁸H. Morito, K. Oikawa, A. Fujita, K. Fukamichi, R. Kainuma, K. Ishida, and T. Takagi, *J. Magn. Magn. Mater.* **290–291**, 850 (2005).

¹⁹K. Oikawa, Y. Imano, V. A. Chernenko, F. H. Luo, T. Omori, Y. Sutou, R. Kainuma, T. Kanomata, and K. Ishida, *Mater. Trans.* **46**, 734 (2005).

²⁰H. Zheng, M. Xia, J. Liu, Y. Huang, and J. Li, *Acta Mater.* **53**, 5125 (2005).

²¹H. Morito, K. Oikawa, A. Fujita, K. Fukamichi, R. Kainuma, and K. Ishida, *Scr. Mater.* **53**, 1237 (2005).

²²T. Kakeshita and T. Fukuda, *Sci. Technol. Adv. Mater.* **7**, 350 (2006).